Optimization of the active absorber scheme for the protection of the Dispersor Suppressor

Magistris M., Santana Leitner M, Vlachoudis V., Ferrari A.

September 5, 2006

Abstract

There are two main types of cold elements in IR7: quadrupole and dipole magnets (MQ and MB). According to predictions, these objects are to lose their superconducting properties if the spurious power densities reach about 1 and 5 $\frac{mW}{cm^3}$, respectively. In order to protect these fragile components, 5 passive absorbers (TCLA) were designed and a systematic study was launched to maximize the shielding efficiency of the absorber system for different configurations (locations and orientations). The TCLA are identical to the secondary collimators (TCS), the only difference is found in the material of the jaw, which, initially, was set integrally to Cu (instead of C) and later included a small W insertion. This report summarizes the survey of cold element protection through TCLA insertion optimization.

Contents

1 Introduction **3**
1.1 Simulations of the IR7 insertion 3
1.2 Scheme of work 3
1.3 Normalization of the results 4
1.4 Candidate Absorbers 4

2 Protection of Q6 **5**

3 Protection of the DS **7**

4 Hadronic shower generated in the active absorbers **8**
4.1 First order calculations 8
4.2 Exact calculations 10

5 Other potentially harmful beam loss scenarios **10**
5.1 Vertical and skew beam loss scenarios at top energy. 12
5.2 Failure/Commissioning modes at top energy 12
5.3 Losses at injection (450 GeV) 13

6 Conclusions **14**
6.1 Dose in MQTLH (MQ6) 14
6.2 Dose in the DS section MQ7-MQ13 14
6.3 Other Scenarios 15

A Data from active absorber optimizations **17**
A.1 Scoring in the MQ's 17
A.2 Scoring in the MB's 17
A.3 Scoring in the MQTLH and MCBC 18
A.4 Re-binning of the results 18
A.5 Peak detection and parsing scripts 19

1 Introduction

1.1 Simulations of the IR7 insertion

The collimation system of the future Large Hadron Collider (LHC) at CERN is a challenging project since the transverse intensities of the LHC beams are three orders of magnitude greater than those of other current facilities. Two insertions (IR3, IR7) of LHC are dedicated to beam cleaning with the design goal of absorbing part of the primary beam halo and of the secondary radiation. These insertions will house 54 movable two-sided collimators, and will be among the most radioactive areas of LHC. The collimators should withstand the deposited power, which for phase I can reach values of about 25 kW in the upstream units ($\sim$3 kW in the jaws).

The tertiary halo that escapes the collimation system in IR7 could heat some fragile elements up to unacceptable levels, if no additional absorber were used. In order to assess the energy deposition in sensitive components, extensive simulations were run with the Monte Carlo cascade code FLUKA[1, 2].

1.2 Scheme of work

The scheme of the simulations has followed the priorities and set-up changes at each point of the project. It was decided firstly to determine the *active* absorbers necessary to shield the critical superconducting coils in the cold section and then to place *passive* absorbers [3] in the straight section for the protection of highly irradiated warm magnets. Next, the heat deposition in the cold part was recomputed to account for the correction introduced by the presence of the active absorbers of the straight section. This calculation contained the corrected description of the TCP, whose active jaws had been extended in the meantime from 20 to 60 cm. From the first calculations it was observed that the horizontal beam loss scenario was the most harmful for the cold magnets so in order to limit the CPU usage, it was the only case considered most of the time. This hypothesis, however, was validated at the end of the decision scheme by checking the doses of the final setup with the vertical and skew beam loss scenarios. Moreover, the irradiation for the injection is computed at the end of the report.

Thus, the simulations are organized as follows:

1. Calculation of heat deposition in cold section without protection, 20 cm TCP.
2. Optimization of active absorbers in the cold section, 20 cm TCP.
3. *Optimization of passive absorbers in straight section, 60 cm TCP.* [3]

4. Re-calculation of heat deposition in cold section with passive absorbers, 60 cm TCP.

5. Refinement of calculations (tertiary halo) and accident cases (secondary collimators off).

1.3 Normalization of the results

The power density $\left[\frac{GeV}{cm^3\ p}\right]$ results obtained from FLUKA simulations were transformed $\left[\frac{W}{cm^3}\right]$ by the following factors $Fn\ \left[\frac{W\ p}{GeV}\right]$:

Top energy, nominal conditions $Loss\ rate = 4.0 \cdot 10^{11}\ \left[\frac{p}{s}\right] \Rightarrow Fn = 57.6$

Injection, nominal conditions $Loss\ rate = 8.6 \cdot 10^{11}\ \left[\frac{p}{s}\right] \Rightarrow Fn = 123.8$

Top energy, TCS failure commissioning $Loss\ rate = 0.15 \cdot 4.0 \cdot 10^{11}\ \left[\frac{p}{s}\right] \Rightarrow Fn = 8.6$

Where the loss rates are given for the 0.1 h beam lifetime assumption at ultimate intensity [4][1,2].

1.4 Candidate Absorbers

Optimum solutions were sought among a set of configurations that resulted from taking several variables into account:

Position of the TCLA. Seven candidate **positions** negotiated with the *beam integration group* were allocated for the TCLA; *A4* and *A6* between the interaction point IP7 and the first downstream dogleg bending magnet MBW.D6L7.B1, *C6* between the two downstream dogleg bending magnets, *E6* and *F6* after the second downstream dogleg bending magnet but upstream of MQ6, and *A7 or B7* between MQ6 and the DS. A primary set of simulations scanned through the efficiency of the first 5 TCL in terms of the dose computed for the MQ6 group and, in particular, for the first subcomponent MQTLH.A6R7.B1.

Orientation of the absorber. Two orientations are considered, *horizontal* and *vertical*.

Jaw Material Both full copper and copper with a tungsten insertion (W) were suggested.

[1] These numbers may have been refined since the completion of our computations.

[2] For coherence with initial compuations, the conversion numbers Fn include a 0.9 factor.

Beam loss scenario, which could be mainly horizontal losses (H), vertical (V) or skew (S).

"Brute-force" examination would have required too much CPU so educated shortcuts were taken once the trends examined.

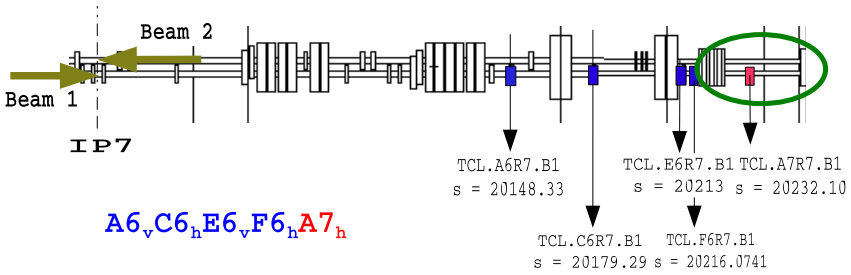

Figure 1: Schematic layout of the finally selected absorbers along IR7 beam1.

2 Protection of Q6

A preliminary set of simulations scanned through the efficiency of the first 5 TCL positions in terms of the power density computed for the coils of the MQ6 group (see appendix, A.3) and, in particular, for the first subcomponent: MQTLH.A6R7.B1[3]. *A4* was soon discarded (too far away), while *A6*, *C6* and *E6* were retained. Moreover, it was verified that an alternating angle scheme was best filtering the showers, so the starting configuration was frozen as $A6_vC6_hE6_v$[4]. Initially, when $5\ \frac{mW}{cm^3}$ was taken as threshold, the 3 TCL alone could comply with specifications ($\rho_E \sim 1.7\ \frac{mW}{cm^3}$), but after the establishment of the more stringent level of $1\ \frac{mW}{cm^3}$, it became clear that a fourth absorber ($F6_h$) would be needed to shield MQTLH.A6R7.B1 with some confidence. The resulting configuration ($A6_vC6_hE6_vF6_h$) indeed reduced the peak density in MQ6 down to about $0.77\ \frac{mW}{cm^3}$, still allowing a relatively scarce margin for contingencies. Improvements were then tentatively looked for by rerunning simulations with W insertions in the Cu jaws. Results proved enormously encouraging, with peak power densities as small as $0.20\ \frac{mW}{cm^3}$.

However, that was not the end of the story. Two major changes took place shortly after: first, passive absorber blocks were introduced in the straight section

[3]NOTE THAT ALL THE FOLLOWING CALCULATIONS CARRY OUT IMPORTANT UNCERTAINTIES AND THAT RESULTS SHOULD BE INTERPRETED QUALITATIVELY AND NEVER LITTERALY.

[4](v) stands for vertical and (h) for horizontal orientation of the TCL.

[5, 6] and, second, the active length of the jaws of the primary collimators was changed from 20 to 60 cm, which finally raised the dose in the MQTLH by a factor 2, up to $0.45\ \frac{mW}{cm^3}$. The results of the successive simulations can be followed in table 1[5].

TCS	TCP	TCL	A4	A6	C6	E6	F6	MQ6
100	20	Cu						850
			h					850
			v					650
				h				550
				v				700
					h			170
					v			300
						h		700
						v		80
				v	h			5.5
					h	v		2.2
				v	h	v		1.7
					h	v	h	1.3
				v	h	v	h	0.7
		W		v	h	v	h	0.2
	60	W		v	h	v	h	0.46
0	60	W		v	h	v	h	30

Table 1: SCENARIO: horizontal losses at top energy and nominal conditions. Power density peaks $[\frac{mW}{cm^3}]$ in the coils of MQTLHA6L1. Last line corresponds to a commissioning scenario where the TCS are retracted and, thus, the power density of 30 $\frac{mW}{cm^3}$ has to be weighted by the 0.15 factor, as explained in 1.3. The two last lines include passive absorbers [5].

† The W insertion in the Cu jaws reduces the heat deposition in the MQTLH group by about 50 %.

† The dose in MQTLH with the 60 cm long TCP jaws is twice as high as that with the 20 cm long jaws.

[5]To get the energy deposition for the commissioning case, apply the factor 0.15 to account for the fact that for this scenario the beam will carry less than 15 % of the nominal intensity.

3 Protection of the DS

The previous situation left one absorber available at *A7* or *B7* to provide extra shielding for the MQ's and MB's of the DS. Simulations were carried out for each of the two positions with horizontal and vertical jaws and the goodness of each solution was judged through the total and peak doses in MQ7-MQ13 and MB.A8R7.B1-MB.C13R7. The best solutions, equivalent within statistical fluctuations, were those containing $A7_h$ or $B7_h$, compared in fig. 2. The magnetic field

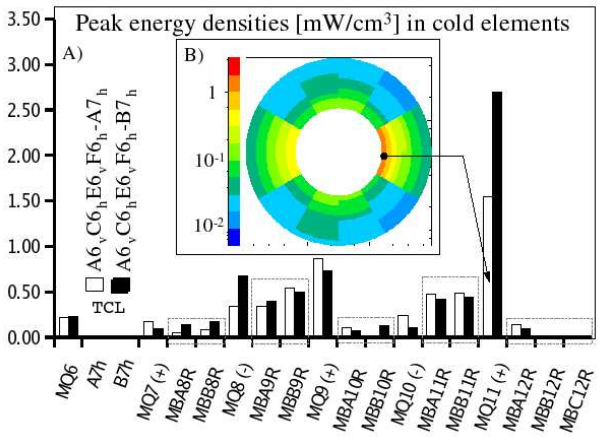

Figure 2: A.) Energy density $[\frac{mW}{cm^3}]$ in MQ and MB for $A7_h$ (□) and for $B7_h$ (■). B.) Energy density in MQ11.

was refined several times for an optimum tracking in the MB's, but the results remained stable in the range of small corrections, which affirmed the confidence in the calculations. Moreover, fig. 2.A seems coherent with the expected beam optics, with a broader horizontal beam (and thus higher doses) in the MB's that follow an h-defocusing quadrupole (-). It is remarked that not only the doses remain mainly under the quench limits, but also the z-derivatives show that the beam delivered beyond IR7 should not be destructive, as proven in [7]. For MQ11 (fig. 2A and B), however, special actions may have to be taken in the future.

Table 3 summarizes the study on peak power densities ($[\frac{mW}{cm^3}]$) in the MBs and MQs for two positions ($B7$, $A7$) and orientations (h, v) of the fifth absorber. Columns 2 and 3 deal with integrally copper TCLA jaws, while the other columns display the result for the W insertion case. From column 5 onwards simulations were performed with the 60 cm active length TCP's. Column 6 describes the accident case when the TCS are retracted, and column 7 shows the contribution of the direct impacts in the TCLA. Column 8 adds up the results of column 5 and column

Absorber	$A4_{v/h}$	$\mathbf{A6}_{v}$	$\mathbf{C6}_{h}$	$\mathbf{E6}_{v}$	$\mathbf{F7}_{h}$	$\mathbf{A7}_{h}$‘	$B7_{v/h}$
Position abs.$[m]$	20022.5	20148.3	20179.3	20213.1	20216.1	20232.1	20243.9
Position-IP7 $[m]$	28.37	153.927	184.801	218.352	220.351	237.698	249.781
Orientation	V/H	V	H	V	V	H	V/H
Half gap $[\mu m]$	$10\,\sigma_{x/y}$	1585	2840	2787	1779	1788	$10\,\sigma_{x/y}$

Table 2: Summary of the properties of the **selected** and *discarded* absorbers.

7.

† The peak energy densities for the horizontal loss scenario are bigger in the objects immediately downstream a h-defocusing MQ.

† The peak energy densities remain below the expected quench limits.

† The most irradiated object is MQ11.

4 Hadronic shower generated in the active absorbers

As discussed in the previous sections, some of the active absorbers have been placed in front of the first superconducting magnets in order to shield them from the hadronic shower generated upstream in the tunnel. The half-gap of the jaws is at 10 σ with respect to the beam profile; this value is relatively high compared to the one of the primary (6 σ) and secondary (7 σ) collimators. Such a large aperture guarantees a fairly low, though non-zero number of primary proton-TCLA collisions. In fact, the showers originated upon the rare beam halo interception events in the TCLA jaws, could have significant impact in the superconducting objects close-by. In order to evaluate this additional risk of magnet quenching, the study could be divided into two steps: estimating the peak energy deposition in the magnet per primary proton and the number of primaries intercepted by the absorber.

4.1 First order calculations

Dedicated FLUKA simulations were run with a source of particles uniformly distributed over the inner (exposed to the beam) thin layer of the absorber jaws. It was found that if the beam losses in the absorber correspond to 0.1% of the total losses in the collimators, then the peak density raised in the superconducting coils would be around 1 $\frac{mW}{cm^3}$, which is comparable to the contribution from the collimator losses.

1	2	3	4	5	6	7	8	
TCPjaws	**20 cm**	20 cm	20 cm	**60 cm**	60 cm	60 cm	60 cm	1
TCLjaws	**Cu**	Cu	**Cu+W**	Cu+W	Cu+W	Cu+W	Cu+W	2
TCS	**ON**	ON	ON	ON	ON	ON	**OFF**	3
5^{th}Absor.	$\mathbf{B7_v}$	$\mathbf{B7_h}$	$\mathbf{A7_h}$	$A7_h$	$A7_h$	$A7_h$	$A7_h$	4
PA:	**OFF**	OFF	OFF	**ON**	ON	ON	ON	5
Source: TC..	**P+S**	P+S	P+S	P+S	**L**	**P+S+L**	**P+L**	6
MQ6	0.77	1.10	0.22	0.45	0.35	0.80	29.9	7
MQ7	*0.46*	*0.50*	*0.18*	*0.12*	*0.21*	*0.33*	*2.4*	8
MBA8	0.10	0.39	0.05	0.07	0.09	0.16	1.7	9
MBB8	0.32	0.38	0.09	0.11	0.04	0.15	0.5	10
MQ8	*0.88*	*0.82*	*0.35*	*0.29*	*5E-3*	*0.29*	*0.4*	11
MBA9	0.60	1.39	0.35	0.63	3E-3	0.63	0.8	12
MBB9	0.54	1.56	0.55	0.67	1E-3	0.67	1.0	13
MQ9	*0.35*	*1.67*	*0.88*	*1.14*	*2E-3*	*1.14*	*2.4*	14
MBA10	0.08	0.32	0.12	0.18	$\sim$0	0.18	0.3	15
MBB10	4E-3	7E-3	0.02	0.03	$\sim$0	0.03	0.1	16
MQ10	*0.16*	*0.57*	*0.24*	*2.34*	*$\sim$0*	*2.34*	*0.3*	17
MBA11	0.37	1.81	0.48	0.65	1E-3	0.65	1.3	18
MBB11	0.38	1.02	0.49	0.60	1E-3	0.60	1.5	19
MQ11	*2.56*	*3.10*	*1.55*	*$\sim$0*	*$\sim$0*	*$\sim$0*	3.7	20
MBA12	0.10	0.28	0.14	0.18	$\sim$0	0.18	0.2	21
MBB12	1E-3	0.08	0.01	0.03	$\sim$0	0.03	$\sim$0	22
MBC12	-	3E-3	$\sim$0	0.01	$\sim$0	0.01	$\sim$0	23
MQ12	*0*	*0*	*0*	*0*	*0*	*$\sim$1E-3*	$\sim$0	24

Table 3: Peak power densities $[\frac{mW}{cm^3}]$ in the DS for the horizontal beam loss scenario at 7 TeV (**lwb**). Five *active* absorbers (**TCL**) are on, $A6_vC6_hE6_vF6_h$ (chosen in sec. 2) + 5^{th} absorber (row 4), and sometimes also the *passive* absorbers (**PA**, see ch.**??**), row 5. As for the loss source (row 6), simulations were first computed for losses originated in the TCP and TCS only. Then the contributions from the TCL were included, i.e. Column 7 = Column 5 + Column 6. Column 8 represents the commissioning case where the TCS are off (a reduction factor of 0.15 needs then to be applied to account for the reduced intensity during commissioning).

4.2 Exact calculations

Only after having frozen the positions of the five active absorbers, the beam tracking codes could be rerun to obtain the new proton interactions. The new file essentially is comparable to the old one, with the exception of a few interaction events in the newly introduced active absorbers[6].

From the fresh interaction file a new source file that included all interactions (in collimators and absorbers) could be generated and the doses could be recomputed as in the previous sections. However, since the fraction of interactions in the absorbers is very little and the statistical fluctuation of the results rather big, it would be quite difficult to tell what is the contribution of the showers coming from interactions in the absorbers to the total peaks in the cold arc. Thus, a set of simulations was launched with a source file filtered exclusively in the active absorbers, and the results were accordingly weighted (to the likeliness of such collisions).

The number of interactions in the absorbers for the given data was 845 out of 1242331 interactions everywhere. The contribution of the showers induced by the proton impacts in the active absorbers, scaled by $\frac{845}{1242331} = 6.8 \cdot 10^{-4}$ appears in the 7^{th} column of table 3 in sec.6. The increase of dose is compatible, though less important, than the one predicted in the first order calculation where the number of impacts in the TCLA was tentatively taken as 0.1% while beam tracking calculations cast 0.07 %

5 Other potentially harmful beam loss scenarios

The first calculations determined that the horizontal loss scenario was the worst in terms of peak dose in the cold section. However, a few variables changed from the initial calculations, and some others were not even considered. For example, the active length of the primary collimators was extended from 20 to 60 cm, passive absorbers were inserted, and the halo showers in the absorbers was included in the beam interaction files. These changes justify to check the final dose also in the vertical beam loss. Other scenarios that are surveyed are those that occur during injection, *failure modes*[7] where the TCS are retracted, and combination of both.

[6] Indeed, for multi-turn computations a particle intercepted in the TCLAs will follow a different path through the "old" elements, so the effect is not exclusively seen in the TCLAs but also, though moderately, in the other objects.

[7] in contrast with the nominal mode.

1	2	3	4	5	6	7	8	9	
$\frac{\mathbf{E[GeV]}}{\mathbf{beam}}$	**7000**	7000	7000	7000	7000	**450**	450	450	1
TCS	**ON**	ON	**OFF**	ON	**OFF**	ON	**OFF**	OFF	2
TCL	**OFF**	**ON**	ON	ON	ON	ON	ON	ON	3
Beam	**Hori**	Hori	Hori	**Vert**	Vert	**Hori**	Hori	**Vert**	4
MQ6	0.370	1.2	29.9	0.3	39.3	∼0.2	5.5	12.5	5
MQ7	*34*	*0.5*	*2.4*	*∼0.1*	*2.6*	*∼0.02*	*0.7*	*<0.9*	6
MBA8	12	0.2	1.7	∼0.5	2.6	∼0.09	0.1	<0.05	7
MBB8	14	0.2	0.5	∼0.1	∼1	∼0.02	<0.11	∼0.05	8
MQ8	*7*	*1.0*	*0.4*	*∼0.01*	*∼5*	*∼0.07*	*∼0.10*	*∼0.07*	9
MBA9	4	0.60	0.8	0.35	1.5	∼0.02	∼0.03	∼0.03	10
MBB9	1.5	1.0	1.0	∼0.5	1.5	∼0.02	∼0.07	∼0.10	11
MQ9	*1.4*	*1.3*	*2.4*	*∼0.4*	*1.7*	*∼0.01*	*∼0.03*	*<0.03*	12
MBA10	0.5	0.4	0.3	∼0.03	∼0.5	<0.02	<0.05	<0.07	13
MBB10	0.01	∼0.02	∼0.1	∼0.3	∼0.02	∼2E-3	<0.05	<0.07	14
MQ10	*1.0*	*0.5*	*0.3*	*∼0.02*	*∼0.5*	*∼0.02*	*∼0.07*	*<0.07*	15
MBA11	1.7	0.7	1.3	0.2	1.8	∼0.01	∼0.05	-	16
MBB11	0.9	0.9	1.02	<0.6	2	∼0.01	∼0.05	∼0	17
MQ11	*8*	*3.7*	*3.8*	*3.5*	*≈7*	*∼0.05*	*∼0.07*	∼0	18
MBA12	-	∼0.4	∼0.3	0.14	0.7	∼2E-3	∼0	∼0	19
MBB12	-	∼5E-3	<0.1	∼0.02	∼1E-3	∼0	0	∼0	20
MBC12	-	∼0	∼0	∼0.005	0	∼0	0	∼0	21
MQ12	*0*	*0*	*0*	*0*	*0*	*0*	*0*	∼0	22

Table 4: Peak energy densities $[\frac{mW}{cm^3}]$ in the DS for injection and top energy (*row 1*), with horizontal or vertical beam losses (*row 4*). Five *active* absorbers (**TCL**), $A6_vC6_hE6_vF6_hA7_h$ (chosen in sec.2, 3) are on or off (*row 3*) with the *passive* absorbers (**PA**, see [5, 6]). *Row 2* distinguishes a failure mode where the TCS are retracted. The loss rate was $8.6 \cdot 10^{11}\ \frac{p}{s}$ at injection, and $4.0 \cdot 10^{11}\ \frac{p}{s}$ at top energy [4].

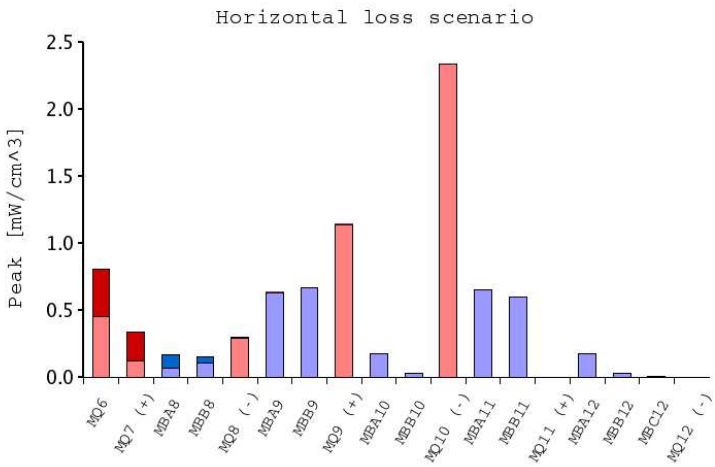

Figure 3: A.) Energy density $[\frac{mW}{cm^3}]$ in MQ and MB for $A6_vC6_hE6_vF6_hA7_h$. Each bar is composed of the contribution from primary and secondary collimators plus that from the active absorbers.

5.1 Vertical and skew beam loss scenarios at top energy.

Table 5 serves to compare the peak power densities in MQTLH6 and MQ7-MQ11 at low beta (7000 GeV/beam) for horizontal, vertical and skew beam loss scenarios at ultimate intensity. The hottest object, MQ11, registers values of about 3.7, 3.6 and 1.1 $\frac{mW}{cm^3}$ for the three cases, respectively. Thus, as anticipated in the early calculations, the horizontal beam loss scenario is the most hazardous one for the DS survival.

5.2 Failure/Commissioning modes at top energy

This section studies a commissioning case where the secondary collimators are open. Thus the active absorbers are left to capture the secondary and tertiary halo. From COLLTRACK [8] calculations, both for the horizontal and vertical loss scenarios at low beta and in failure mode, the number of interactions in the active absorbers can rise by up to 5 orders of magnitude with respect to those in nominal operation. In any case, the biggest source of showers within the active absorbers is TCLAC6.

In nominal operation, where the active absorbers count no more than 1 ‰ of the total interactions, the contribution of their showers in the peak energy densities of

1	2	3	4
Loss	**hori**	**vert**	**skew**
MQ6	1.2	0.25	0.20
MQ7	*0.5*	*0.1*	*0.1*
MBA8	0.2	0.3	0.05
MBB8	0.2	0.03	0
MQ8	*1.0*	*0.20*	*0.03*
MBA9	0.60	0.22	0.23
MBB9	1.0	0.27	0.36
MQ9	*1.3*	*0.29*	*0.59*
MBA10	0.4	0.06	0.05
MBB10	$\sim$0.02	0.12	0.01
MQ10	*0.5*	*0.001*	*0.00*
MBA11	0.7	0.39	0.23
MBB11	0.9	0.25	0.30
MQ11	*3.7*	3.6	1.1

Table 5: Peak energy densities $[\frac{mW}{cm^3}]$ in the DS at top energy and nominal conditions for three beam loss scenarios: **hori**zontal, **vert**ical and **skew**.

MQ6 and MQ7 reach 50 %[8]. Thus, the failure mode could be expected to quench the magnets. However, a specification for this commissioning scenario is that the loss rate stays below 15 % of the nominal loss (see section 1.3 on page 4).

Simulations for the vertical loss scenario cast the results represented in fig. 3.

5.3 Losses at injection (450 GeV)

At injection the beam spot is broader and the loss rates are higher. The collimators and absorbers are adapted to the beam *sigma* at each location and energy. Figure 5 shows that the power densities deposited in the cold section for horizontal losses at injection with all protection devices (collimators) on are well below those registered at top energy (like those shown in fig 4).

More results can be found in the three rightmost columns of table 4.

[8] As shown in figure 3.

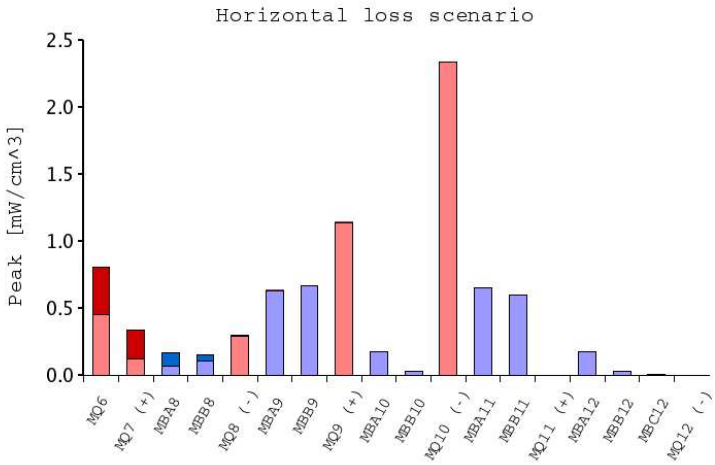

Figure 4: Energy density $[\frac{mW}{cm^3}]$ in MQ and MB for $A6_vC6_hE6_vF6_hA7_h$ with a horizontal beam loss scenario. Tertiary halo is included, but TCS are retracted.

6 Conclusions

6.1 Dose in MQTLH (MQ6)

The results of the discussions (see sec.2) of peak energy depositions in MQTLHA6 are shown in table 1.

† The W insertion in the Cu jaws reduces the heat deposition in the MQTLH group by about 50 %.

† The dose in MQTLH with the 60 cm long TCP jaws is twice as high as that with the 20 cm long jaws.

6.2 Dose in the DS section MQ7-MQ13

The results of the discussions (see sec.3) of peak energy depositions in MQ7-MQ13 are shown in table 3.

† The W insertion in the Cu jaws reduces the heat deposition in the first cold objects by about 50 %.

† The dose in DS with the 60 cm long TCP jaws is comparable to that with the 20 cm long jaws.

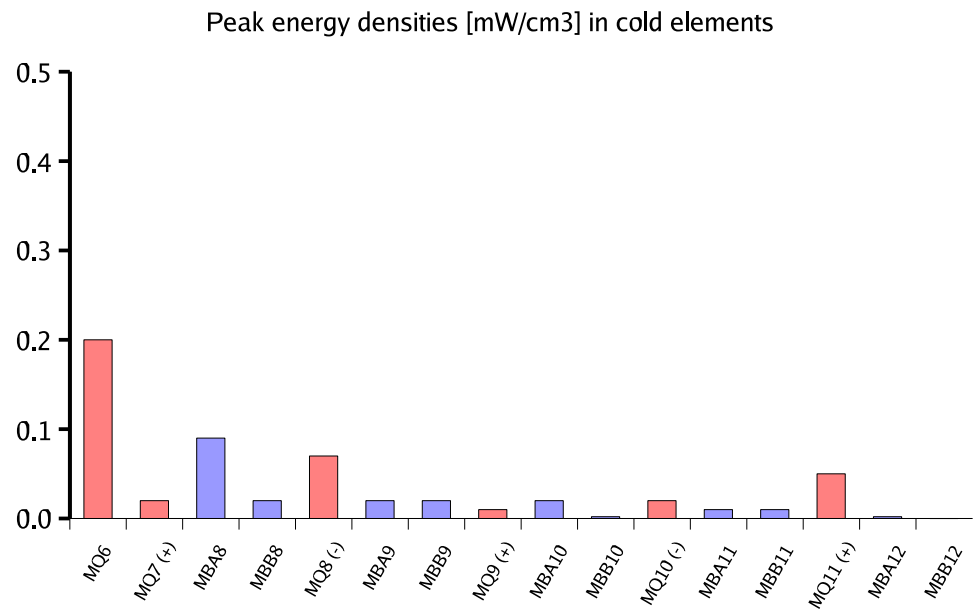

Figure 5: Energy density $[\frac{mW}{cm^3}]$ in MQ and MB for $A6_vC6_hE6_vF6_hA7_h$ with a horizontal beam scenario at injection energy. Tertiary halo is included.

† The contribution of the direct beam impacts in the active absorber multiplies by 2 to 3 the peak energy densities in the MQ6, MQ7 and MBA8, then it damps immediately.

6.3 Other Scenarios

From the results of 5, we can conclude the following (look at table 4) :

† The peak power densities at controlled injection (TCS and TCL on) do not compromise the super-conduction in the magnets ($p_I < 0.35\ \frac{mW}{cm^3}$). However, the values are much larger than those that would be obtained by simply rescaling the results of top energy losses with the energy, e.g. in MQ6 $(p_T = 1.4\ \frac{mW}{cm^3}) \cdot \frac{450}{7000} << p_I$, due to the fact that the beam spot is broader (compare *columns 3* and *7*).

† The failure mode in which the secondary collimators (TCS) are retracted (*columns 2, 6, 8* and *9*) would produce a quench in Q6 ($p_{la} \simeq 30\ \frac{mW}{cm^3}$) at top energy and most likely also at injection ($p_{ia} \simeq 12.5\ \frac{mW}{cm^3}$) for full loss intensity, but not for 15 % of the nominal loss rate. The first three magnets

(MQ6, MQ7, MBA8) absorb most of the additional radiation so that the effect damps quickly and the tail of the DS is not affected by the failure modes.

† The failure mode in which the jaws of the active absorbers (TCL) are retracted (*column 2*) would be catastrophic, the peak density in MQ6 reaching 700 $\frac{mW}{cm^3}$.

† At top energy and normal operation, the horizontal beam loss scenario is neatly more harmful than the vertical one. The most irradiated objects in both cases are MQ11 (*5.0* and *3.8* $\frac{mW}{cm^3}$, respectively) and MQ6 (*1.4* and *0.3* $\frac{mW}{cm^3}$, respectively).

A Data from active absorber optimizations

A.1 Scoring in the MQ's

USRBIN 28 makes a radial-z scoring (10 radial divisions, 12 angular and 31 longitudinal) of the energy deposited in MQ7R-MQ13R (7 bins)

```
***** MQ.7R7.B1
** 7. Beam 1, coil C5B1COIL
USRBIN          11.    ENERGY     -28.0       6.       0.      155.MQ7R
USRBIN        2.80       9.7      -155.      10.      12.       31.&
**
***** MQ.8R7.B1
** 7. Beam 1, coil C5B1COIL
USRBIN          11.    ENERGY     -28.0       6.       0.      155.MQ8R
USRBIN        2.80       9.7      -155.      10.      12.       31.&
...
```

A.2 Scoring in the MB's

USRBIN 32 makes a radial-z scoring (10 radial divisions, 9 angular and z divisions every 17.85 cm) of the energy deposited in MBA8R, MBB8R; MBA9R, MBB9R; MBA10R, MBB10R; MBA11R, MBB11R; MBA12R, MBB12R, MBC12R; MBA13R, MBB13R, MBC13R[9]. The magnets have a bend, which in the FLUKA input has been introduced by chopping the MB's in three straight sections. Consequently, the USRBIN are also divided into three bins for each magnet, one for the first quarter, another for the medium half and the last for the last quarter of the magnet. In total there are $3 \cdot 14 = 42$ bin inside USRBIN 32. It should be pointed out that the axis of the cylindrical mesh is straight while the magnet sections have a small angle (to provide the bending), as illustrated in fig.6.

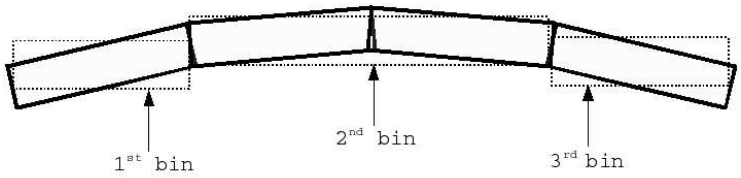

Figure 6: Sketch of the MB FLUKA implementation in 4 straight cylinders and of the corresponding scoring meshes, 1 and 3 for the extremes and 2 for the central part.

```
****  MB.A8R7.B1
* 1. Beam 1, section a
USRBIN          11.    ENERGY     -32.0      6.00       0.     -357.MBA8R
```

[9]Note that MB12 and MB13 are triplets.

```
USRBIN         2.5         10.04       -715.         10.          9.          40.&
* 1. Beam 1, section b and c
USRBIN          11.       ENERGY       -32.0         6.00         0.         357.MBA8R
USRBIN         2.5         10.40       -357.         10.          9.          80.&
* 1. Beam 1, section  d
USRBIN          11.       ENERGY       -32.0         6.00         0.         715.MBA8R
USRBIN         2.5         10.04        357.         10.          9.          40.&
*
**** MB.A8R7.B1
* 1. Beam 1, section a
USRBIN          11.       ENERGY       -32.0         6.00         0.        -357.MBB8R
USRBIN         2.5         10.04       -715.         10.          9.          40.&
* 1. Beam 1, section b and c
USRBIN          11.       ENERGY       -32.0         6.00         0.         357.MBB8R
USRBIN         2.5         10.40       -357.         10.          9.          80.&
* 1. Beam 1, section  d
USRBIN          11.       ENERGY       -32.0         6.00         0.         715.MBB8R
USRBIN         2.5         10.04        357.         10.          9.          40.&
...
```

A.3 Scoring in the MQTLH and MCBC

USRBIN 33 makes a radial-z scoring (1 radial divisions, 20 angular 13 z divisions) of the energy deposited in MQTLH.A6R7.B1, MQTLH.B6R7.B1, MQTLH.C6R7.B1, (some other bins exist but are usually inactive) and also of the energy in MCBCV6R.

```
* 1. Beam 1, coil C1B1COIL
USRBIN          11.       ENERGY       -33.0        3.57         0.          65.MQTLHA6R
USRBIN        2.32         9.7         -65.          1.          20.          13.&
...
*** MCBCV.6R7.B1
* 13. Beam 1, coil C2B1COIL
USRBIN          11.       ENERGY       -33.0        3.85         0.          45.MCBCV6R
USRBIN        2.82         9.7         -45.          1.          20.           9.&
...
```

A.4 Re-binning of the results

The loss events in the DS are so rare that collecting statistics in a fine mesh results into a blurry/spiky image. In order to stabilize the results, these were re-binned into bigger portions of volume. The re-binning factors were chosen as a compromise statistics/peak resolution.

The compression factors (*o*ld vs. *n*ew) where the following:

- For USRBIN 28 ϕ_o/ϕ_n=4
- For USRBIN 32 z_o/z_n=2, ϕ_o/ϕ_n=3
- For USRBIN 33 MQTLH ϕ_o/ϕ_n=5

- For USRBIN 33 MCBC

The script *rebin.sh* produces a list with all the results in the given directory and runs the program *ubredu_stat* with the re-binning factors specified above. The '.rb" suffix is appended to the re-binned output files. Then *anMBMQ.sh* can be used normally by just specifying to use the re-binned results.

A.5 Peak detection and parsing scripts

The script *anMBMQ.sh* produces the table of *LatticeWatt* and the tables of peak energy depositions *results*. This is done by summing up the different results, re-binned (R) or original (O) and thereafter parsing values from the summary files *usrbin* or calling the *EnLattice.pl* program.

A typical table of results is shown below:

```
/home/LHC/IR7/TCP60new/NoTCS/hori/COLD_SECTION
Number of simulations: 55
******* Straight Section *************
**    * MQTLHA6R ******************
      * max heat in coil:........     1.340 mW (+-     25.0 %)
      * Total heat in the coil:..     0.62  W  (+-    10.00 %)
      * heat in MQ:..............     2.34  W  (+-    12.49 %)
**    * MQ6 group *****************
   MQTLHA6R      2.34 (+-    12.49 %) W
   MQTLHB6R      0.67 (+-     6.79 %) W
   MQTLHC6R      0.53 (+-     7.28 %) W
   MQTLHD6R      0.34 (+-     8.56 %) W
   MQTLHE6R      0.27 (+-     8.72 %) W
   MQTLHF6R      0.30 (+-    11.79 %) W
  -----------------------------------
      TOTAL      3.88 (+-     7.72 %) W
******* Curved Section *************
Total energy in coils and magnets of MQ[7-11]R.
   MQ7    | max: 0.565 (+-90.9%)  |   4.189e-01  +- 31% |  Total: 0.785 W    +- 18.8 %
   MQ8    | max: 3.078 (+-93.7%)  |   1.034e+00  +- 24% |  Total: 1.720 W    +- 15.7 %
   MQ9    | max: 2.967 (+-24.8%)  |   4.309e+00  +- 17% |  Total: 7.737  W   +- 10.5 %
   MQ10   | max: 0.009 (+-100.0%) |   5.716e-04  +- 85% |  Total: 0.0134 W   +- 62.8 %
   MQ11   | max: 9.940 (+-28.5%)  |   4.968e+00  +- 16% |  Total: 8.234  W   +- 10.4 %
Total energy in coils and magnets of MB[A-B][8-11]R.
   MBA8R   | max: 0.350 (+-100.0%) 0.684 (+-99.2%)  0.152 (+-97.2%)  | 1:MB_CO1C2:  ...
   MBB8R   | max: 0.353 (+-99.9%)  0.246 (+-99.9%)  0.111 (+-96.4%)  | 2:MB_CO1C2:  ...
   MBA9R   | max: 1.841 (+-35.5%)  1.865 (+-44.9%)  1.549 (+-43.8%)  | 3:MB_CO1C2:  ...
   MBB9R   | max: 4.045 (+-22.1%)  3.353 (+-22.8%)  1.948 (+-23.7%)  | 4:MB_CO1C2:  ...
   MBA10R  | max: 0.257 (+-99.0%)  0.485 (+-93.5%)  0.163 (+-61.0%)  | 5:MB_CO1C2:  ...
   MBB10R  | max: 0.033 (+-100.0%) 0.095 (+-100.0%) 0.070 (+-100.0%) | 6:MB_CO1C2:  ...
   MBA11R  | max: 2.802 (+-43.0%)  1.654 (+-29.7%)  2.161 (+-32.4%)  | 7:MB_CO1C2:  ...
   MBB11R  | max: 3.220 (+-29.4%)  1.333 (+-25.0%)  1.775 (+-28.8%)  | 8:MB_CO1C2:  ...
```

The table of results displays the peak energy density and the total energy in the coil of MQTLHA6R, as well as the total energy in the full magnet A6, B6, C6, D6, F6, E6 and F6 and the sum of all (with the corresponding statistical errors in %).

As for MQ 7-11 in the cold section, a first column shows the peak energy density, and the last two columns display the total energy in the coils and in the full magnets. Something similar is done for the MB magnets, but in this case three peaks of density of energy per magnet are printed, corresponding to the three subsections of the coils (approach to the bending of the magnets).

References

[1] A. Fassò, A. Ferrari, S. Roesler, P.R. Sala, G. Battistoni, F. Cerutti, E. Gadioli, M.V. Garzelli, F. Ballarini, A. Ottolenghi, A. Empl, and J. Ranft. The physics models of FLUKA: Status and recent developments. In *Computing in High Energy and Nuclear Physics 2003 Conference (CHEP2003), La Jolla, CA, USA, March 24-28, 2003*, volume arXiv:hep-ph/0306267, March 2003.

[2] A. Fassò, A. Ferrari, J. Ranft, and P.R. Sala. *FLUKA: a multi-particle transport code*. CERN, INFN, SLAC, 2005.

[3] M. Magistris, M. Santana-Leitner, V. Vlachoudis, and A. Ferrari. Optimization of the active absorber scheme for the protection of the dispersor supressor. Technical report, CERN-AB-ATB, 2006.

[4] Lamont M. Estimates of annual proton doses in the lhc. Lhc project note, CERN AB/OP, October 2005. 375.

[5] M. Santana-Leitner, M. Magistris, V. Vlachoudis, and A. Ferrari. Protection of warm elements at IR7. passive absorbers and collimators. Technical report, CERN-AB-ATB, 2006.

[6] R. Assmann and A. Ferrari. Passive absorbers and increase of inter-distance between d3 modules in IR7. Engineering change request - class i, CERN, February 2006.

[7] M. Brugger M., F. Cerutti F, M Santana-Leitner, V. Vlachoudis, and A. Ferrari. Transmission of losses out of ir7. Technical report, CERN-AB-ATB, 2006.

[8] G. Robert-Demolaize, R. Assmann, S. Redaelli, and F. Schmidt. A new version of sixtrack with collimation and aperture interface. In Particle Accelerator Conference 05, editor, *PAC05 proceedings*, CERN CH-1211 Geneva-23 Switzerland, 2005. CERN. Published.